Received: 24 July 2023 | Accepted: 15 November 2023

DOI: 10.1111/jpy.13418

RESEARCH ARTICLE

Environment-dependent metabolic investments in the mixotrophic chrysophyte *Ochromonas*

Gina S. Barbaglia[1] | **Christopher Paight**[1] | **Meredith Honig**[1] | **Matthew D. Johnson**[2] | **Ryan Marczak**[1] | **Michelle Lepori-Bui**[1,3] | **Holly V. Moeller**[1]

[1]Department of Ecology, Evolution, and Marine Biology, University of California—Santa Barbara, Santa Barbara, California, USA

[2]Biology Department, Woods Hole Oceanographic Institution, Woods Hole, Massachusetts, USA

[3]Washington Sea Grant, University of Washington, Seattle, Washington, USA

Correspondence
Gina Barbaglia and Holly Moeller, Department of Ecology, Evolution, and Marine Biology, University of California—Santa Barbara, Santa Barbara, CA 93106, USA.
Email: barbaglia@ucsb.edu and holly.moeller@lifesci.ucsb.edu

Funding information
Division of Ocean Sciences, Grant/Award Number: OCE-1851194; Simons Foundation, Grant/Award Number: Award 689265

Editor: M. Roleda

Abstract

Mixotrophic protists combine photosynthesis and phagotrophy to obtain energy and nutrients. Because mixotrophs can act as either primary producers or consumers, they have a complex role in marine food webs and biogeochemical cycles. Many mixotrophs are also phenotypically plastic and can adjust their metabolic investments in response to resource availability. Thus, a single species's ecological role may vary with environmental conditions. Here, we quantified how light and food availability impacted the growth rates, energy acquisition rates, and metabolic investment strategies of eight strains of the mixotrophic chrysophyte, *Ochromonas*. All eight *Ochromonas* strains photoacclimated by decreasing chlorophyll content as light intensity increased. Some strains were obligate phototrophs that required light for growth, while other strains showed stronger metabolic responses to prey availability. When prey availability was high, all eight strains exhibited accelerated growth rates and decreased their investments in both photosynthesis and phagotrophy. Photosynthesis and phagotrophy generally produced additive benefits: In low-prey environments, *Ochromonas* growth rates increased to maximum, light-saturated rates with increasing light but increased further with the addition of abundant bacterial prey. The additive benefits observed between photosynthesis and phagotrophy in *Ochromonas* suggest that the two metabolic modes provide nonsubstitutable resources, which may explain why a tradeoff between phagotrophic and phototrophic investments emerged in some but not all strains.

KEYWORDS
metabolism, mixoplankton, phagotrophy, photoacclimation, photosynthesis, plasticity, tradeoffs

INTRODUCTION

Mixotrophs, organisms that obtain energy and nutrients through a combination of photosynthesis and phagotrophy (Stoecker, 1998), are increasingly recognized as crucial components of aquatic food webs and regulators of global biogeochemical cycles (Caron, 2016; Estep et al., 1986). Mixotrophy is common among a diverse group of planktonic protists and may account for over 80% of total chlorophyll and up to 95% of bacterivory in marine systems (Zubkov & Tarran, 2008). In freshwater systems, mixotrophic flagellates are the major grazers

Abbreviations: CCMP, culture collection of marine phytoplankton; CTAB, cetyltrimethylammonium bromide; CUE, carbon use efficiency; ETR, electron transport rate; FLB, fluorescently labeled bacteria; NCMA, National Center for Marine Algae and Microbiota; PCR, polymerase chain reaction.

during winter and spring blooms in eutrophic communities (Sanders et al., 1989); they are also the dominant grazers in oceanic oligotrophic gyres (Hartmann et al., 2012). Mixotrophic protists also impact carbon cycling by acting as either carbon sinks as they absorb CO_2 through photosynthesis or carbon sources as they release CO_2 through aerobic respiration of ingested material (Jassey et al., 2015; Wilken et al., 2014).

In aquatic ecosystems, mixotrophy is classified as either constitutive or nonconstitutive (Stoecker, 1998). Here, we focus on constitutive mixotrophs that possess permanently incorporated, vertically transmitted plastids rather than on nonconstitutive mixotrophs that transiently obtain photosynthesis by hosting photosynthetic endosymbionts or stealing them from algal prey (Mitra et al., 2016; Stoecker, 1998). The nutritional strategies of constitutive mixotrophs are highly variable, existing on a spectrum ranging from primarily phototrophic to primarily phagotrophic (Stoecker, 1998). For example, among the constitutively mixotrophic chrysophytes currently classified within the *Ochromonas* genus, the *Ochromonas* strain SEM is primarily phagotrophic, while *O. pinguis* is an obligate mixotroph using phototrophy as a primary metabolic strategy with phagotrophy as a supplemental strategy (Holen, 2010). Studies have shown that *Ochromonas* strains may need phagotrophy as a supplemental strategy in order to meet their phosphorus demand (Foster & Chrzanowski, 2012; Schmidtke et al., 2006). Environmental conditions such as light, temperature, prey availability, and external inorganic nutrients can affect which metabolic strategy is favored (Lie et al., 2018).

Phenotypic plasticity, including mixotroph adjustments in metabolic mode, allows organisms of the same genotype to adjust their physiology, physical attributes, or other aspects of their phenotype in response to changing environmental conditions (Li et al., 2021; Wilken et al., 2014, 2020). Such adjustments can help organisms economize on metabolic investments. For example, many photosynthetic organisms exhibit photoacclimation: They adjust their chlorophyll production in response to a change in photon flux density and spectral distribution (Falkowski, 1980). In high light conditions, photoacclimation allows cells to preserve metabolic resources and reduce photodamage (including through the production of secondary pigments; Wilken et al., 2019). As light availability decreases, photoautotrophs increase investments in photosynthetic machinery, such as light-harvesting complexes and the ratio of reaction centers (Falkowski et al., 1981; MacIntyre et al., 2002; Sukenik et al., 1988), to increase the proportion of photons that they capture. Thus, in photoautotrophs, chlorophyll-*a* pigment content and photosynthetic efficiency are generally decreasing functions of light availability (Falkowski, 1980; MacIntyre et al., 2002). In order to undergo photoacclimation, cells must register a change in light intensity, transduce this signal through the electron transport chain, and eventually alter gene expression of photosynthetic machinery (Escoubas et al., 1995).

However, mixotrophs have two metabolic modes, which may complicate their investment strategy. In photosynthetic eukaryotes, biomass investments in photosynthetic machinery are significantly more costly (ca. 50% of the cell's biosynthetic energy costs) than investments in phagotrophic machinery (ca. 10%; Raven, 1997). Because energy, carbon, and cytoplasmic space dedicated to plastids (photosynthetic machinery) cannot be used for digestive vacuoles (phagotrophic machinery), mixotrophs are expected to change their metabolic strategy based on resource limitation (Berge et al., 2017; Våge et al., 2013; Ward et al., 2011). For example, some *Ochromonas* species rely heavily on heterotrophy for growth (Sanders et al., 2001) and will only use phototrophy under prey-limiting conditions (Andersson et al., 1989; Holen, 2010). The mixotrophic chrysophyte *Poterioochromonas malhamensis* also reduces photosynthetic machinery when prey is available in sufficient quantities (Sanders et al., 1990). However, adjustments in metabolic strategy are constrained by fundamental resource demands: While photosynthesis can produce carbon, phagotrophy can generate both carbon and nitrogen (as well as other elemental resources). Thus, depending on their ability to take up inorganic nutrients, some mixotrophs may be obligately phagotrophic to obtain noncarbon resources. These dynamic metabolic responses to changing environmental conditions complicate our ability to predict mixotrophs' functional role in larger food webs and biogeochemical cycles (Fischer et al., 2022; Jansson et al., 1996).

In this study, we used marine members of the constitutively mixotrophic genus *Ochromonas* to test how resource availability affected the cell's metabolic strategy. Working with eight strains of *Ochromonas*, we quantified growth and metabolic investments as a function of light, bacterial prey availability, and phylogeny. We compared the importance of phagotrophy and phototrophy to growth and analyzed how both cellular investments (i.e., chlorophyll content and attack rates) and metabolic rates (i.e., carbon fixation rates and bacterial ingestion rates) changed in response to resource availability. We chose to test multiple strains of *Ochromonas* because we expected them to occupy different positions along the mixotrophic spectrum and therefore have varying metabolic responses. Our data suggested that for this constitutive mixotrophic genus, all strains tended to upregulate photosynthetic machinery when light was limiting and increase attack rates when bacterial abundances were low. Photosynthesis and phagotrophy generally produced additive benefits, suggesting some resource complementarity across metabolic modes. However, despite the close relatedness of the eight strains, they exhibited varying metabolic strategies under the same resource constraints.

MATERIALS AND METHODS

Cultures and maintenance conditions

To contrast the performance of multiple marine *Ochromonas* strains, we used eight marine strains available from the National Center for Marine Algae and Microbiota (NCMA, Bigelow Laboratory, East Boothbay, ME) culture collection: CCMP 584, 590, 1148, 1150, 1391, 1392, 1393, and 2951. These strains were originally collected from three sites across the world (Figure S1 in Appendix S1 in the Supporting Information). Strain CCMP 1391 is a facultative heterotroph that can survive in the absence of prey (Moeller et al., 2019); CCMP 1393 is an obligate mixotroph that requires both light and prey (Wilken et al., 2020); and CCMP 2951 is a facultative phototroph that requires prey but can grow in darkness (Wilken et al., 2020). However, little is known about the metabolic investment strategies of the other five strains. All *Ochromonas* stock cultures were maintained in K medium (Keller et al., 1987) created by adding premixed nutrients (ordered from the NCMA) to 0.2 μm filtered, autoclaved Santa Barbara coastal sea water. See Appendix S1: Table S1 for a list of final nutrient concentrations in K medium. Stock cultures were maintained at 24°C under a 12:12 h light:dark cycle with illumination from above.

Experimental design

We conducted a fully factorial experiment in which eight *Ochromonas* strains were acclimated to two prey conditions (high or low bacteria) and seven light levels (0, 15, 25, 50, 75, 100, and 150 μmol photons $\cdot$ m^{-2} $\cdot$ s^{-1}) created using a combination of mesh screening and varied shelf proximity to light sources in incubators (Figure 1). To create high prey conditions, a single autoclaved rice grain was added to each *Ochromonas* culture, acting as a persistent food source for bacteria (rice grains were undiminished in size throughout the course of each experiment). *Ochromonas* maintained in low prey conditions were grown with no rice amendment. We determined the abundance of free-living bacteria in cultures by plating exponentially growing *Ochromonas* cultures on Difco Marine Broth 2216 (Difco Laboratories, Sparks, MD, USA) agar plates and enumerating colony forming units. There was a ca. 20 fold increase in bacterial concentration in high prey relative to low prey conditions (Appendix 1: Figure S2). Each stock culture strain was maintained under experimental light and prey conditions for at least 30 days prior to initiation of an experiment in order to allow full acclimation to environmental conditions. After this acclimation period, high-prey experiments were initialized by adding a stock culture volume of 0.1–15 mL of K media

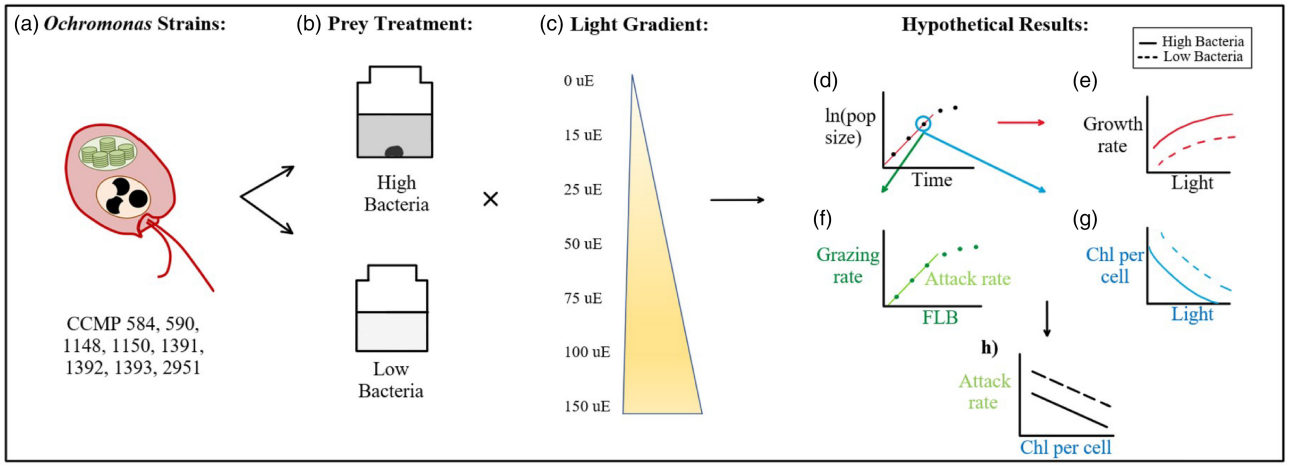

FIGURE 1 Diagram of experimental design. (a) Eight marine *Ochromonas* strains originally collected from three sites across the world were grown in culture. (b) The eight strains were acclimated to high bacterial (high prey) and low bacterial (low prey) conditions. High prey cultures were grown with a single grain of autoclaved rice to provide bacteria with a carbon source. Low prey cultures lacked a carbon source for bacteria. (c) Each experimental culture was maintained over a light gradient of seven different light levels (0, 15, 25, 50, 75, 100, 150 μmol photons $\cdot$ m^{-2} $\cdot$ s^{-1}) created using a combination of mesh screening and varied shelf proximity to light sources in incubators. Three biological replicates were run for each experiment. (d) We predict that the natural log of population size over time will exponentially increase, then begin to plateau. Growth rate was calculated as the slope of a line fit to the natural log of population size over time. Chlorophyll per cell and grazing rate were calculated from a specific point in time. (e) We predict that the growth rate of *Ochromonas* strains will increase with light level and prey availability. (f) We predict that the grazing rate will increase as more prey is available. Attack rate (which is the slope of a line tangent to the functional response curve at low-prey densities) was extracted from functional response curves fit to the data (see *Methods*). (g) Chlorophyll per cell is expected to decrease with increasing light and prey availability. (h) We expect there will be a tradeoff between investments in photosynthesis (Chlorophyll per cell) and phagotrophy (attack rate).

amended with a rice grain, and low-prey experiments began with an inoculation of 0.5 mL stock culture. We ran all experiments (8 strains × 2 feeding regimes × 7 light levels = 112 experiments) in triplicate in 25-mL single-use suspension culture flasks.

Each experiment ran for an average of 20 days (at least 10 days in high-resource conditions and as long as 30 days in low-resource conditions due to lower growth rates when bacteria and light were limiting), in which sampling began the day after inoculation and continued daily, Monday–Friday, while populations were in exponential growth. At each daily sampling, live cell density (in cells per mL) was measured using a Guava easyCyte flow cytometer (Luminex Corporation, Austin, USA), which distinguishes *Ochromonas* cells based on forward scatter (a proxy for cell size) and red fluorescence (a measure of photosynthetic pigmentation). Growth rates were calculated as the slope of a line fit to the natural log of population size over time. To ensure that maximum growth rates were calculated, we excluded any late timepoints at which population growth was slowing due to resource limitation (Figure 1d).

Photophysiology measurements

Photosynthetic efficiency (*Fv*/*Fm*) and electron transport rate were measured using a mini Fluorescence Induction and Relaxation (FIRe) system (custom built by M. Gorbunov, Rutgers University, New Brunswick, NJ, USA). After mixotroph cells were dark acclimated for 15 min photosynthetic efficiency was measured as the proportion of active photosynthetic systems to total photosynthetic systems. Electron transport rates were measured at fifteen light levels spaced between 0 and 700 μmol photons · m^{-2} · s^{-1} (Gorbunov & Falkowski, 2005). These data were used to compute photosynthetic rates at growth irradiance by fitting the equations of Jassby and Platt (1976) using nonlinear least squares regression (R function nls):

$$\mathrm{ETR} = P_{\max} \cdot \tanh\left(\frac{\alpha \cdot I}{P\max}\right).$$

In this equation, ETR is a function of the maximum electron transport rate (P_{max}), the initial slope of ETR with respect to light (α), and the irradiance (I).

Following Lepori-Bui et al. (2022), we converted electron transport rates (electrons per chlorophyll-*a* per second) to per-chlorophyll carbon fixation rates ($P_{I.chl}$) based on the assumption of a quantum yield of oxygen evolution of 0.25 (four electrons needed per molecule of O_2) and a photosynthetic quotient of 1.4 moles O_2 produced per mole CO_2 fixed (Lawrenz et al., 2013; Laws, 1991). Because we did not measure quantum yields or photosynthetic quotients of our mixotrophs directly, this calculation assumes that these parameters did not vary with resource availability.

We measured chlorophyll-*a* as our proxy for mixotroph photosynthetic investment. More specifically, chlorophyll content serves as a measure of a cell's investment in light capture machinery, though investments in downstream C fixation machinery may not always be proportional in mixotrophs. Chlorophyll-*a* was extracted by filtering a known volume of culture onto a GF/F filter (Whatman Part No. 1825-025, Whatman 228 Cytiva, Marlborough, MA, USA) and extracting in 5 mL of 90% acetone (10% MilliQ water) overnight at –20°C. We used a Trilogy fluorometer with a 460 nm LED (Turner Designs, San Jose, CA, USA) to quantify chlorophyll in the extraction. We computed cellular chlorophyll content (chl_{cell}) by dividing total extracted chlorophyll by the number of *Ochromonas* cells filtered (based on flow cytometric counts of cell density performed at the same time as the chlorophyll sample was collected; see *Experimental design* above).

Prey consumption

For each experimental culture exhibiting positive growth, we generated grazing functional response curves following methods previously established in our lab (Lepori-Bui et al., 2022). Briefly, we offered *Ochromonas* heat-killed fluorescently labeled bacteria (FLB; *Escherichia coli* – K-12 strain—Bioparticles®, Alexa 204 Fluor®488 conjugate, Molecular Probes, Invitrogen, Waltham, MA, USA) as prey. The FLB were introduced to *Ochromonas* cultures and sterile seawater controls in a range of concentrations from 0 to 2×10^6 cells · mL^{-1}. After 45 min of grazing, *Ochromonas* and FLB concentrations were quantified on a Guava flow cytometer, using forward scatter, red-fluorescence, and yellow-fluorescence measurements to distinguish between *Ochromonas* and FLB. We computed ingestion using the methods of Jeong and Latz (1994) by comparing prey abundance in predator-free controls to prey abundance in *Ochromonas* treatments (Jeong & Latz, 1994). We fit both Holling Type I (linear) and Holling Type II (saturating) functional response curves to estimate the grazing rates as a function of light and prey availability. We used the Akaike Information Criterion to select the best-fitting model. In most cases, a Type II functional response was the best fit to the data. We extracted attack rates (a.k.a. "clearance rates," in units of mL per *Ochromonas* per hour) and computed grazing rates (a.k.a. "ingestion rates," in units of bacteria per *Ochromonas* per day; estimated based on free-living bacterial abundances in the cultures) from the best functional response fit.

Cellular carbon and nitrogen content

Ochromonas cultures from 15 and 150 μmol photons · m^{-2} · s^{-1} light treatments were prepared for carbon (C) and nitrogen (N) content analysis by filtration of 10 mL of culture onto precombusted GF/F filters (Whatman Part No. 1825-025 Whatman Cytiva, Marlborough, MA, USA). Filters were sent to the UCSB Marine Science Institute Analytical Lab (Santa Barbara, CA, USA) for acidification, which removed inorganic carbonates, and then analysis for cellular carbon and nitrogen content on an elemental analyzer (Control Equipment Corp. CEC 440HA, Chelmsford, MA, USA).

Quantifying investments, carbon yields, and carbon use efficiency

To quantify mixotroph investments in phototrophy and phagotrophy, and the contributions of these investments to mixotrophic growth, we scaled all measurements to mixotroph carbon biomass. To find cells' capacity for photosynthesis, we first normalized cellular chlorophyll-*a* (in pg chl-*a* per cell) to cellular carbon C_{cell} (in pg C per cell) to obtain chl-a_C (in units of mg chl-*a* per g C):

$$\text{chl}-a_C = \frac{\text{chl}-a_{cell}}{C_{\text{cell}}} * \frac{1000\ \text{mg}}{\text{g}} \tag{1}$$

To calculate the rate of carbon fixation via photosynthesis, we multiplied the per-chlorophyll photosynthetic rate ($P_{I.chl}$; see above, in units of grams C fixed per gram chl-*a* per hour) by chlorophyll content and converted the result to a daily rate by multiplying by 12 h (the number of hours of light the *Ochromonas* cultures experienced; note that this assumes constant photosynthetic rates during the entire light period) to obtain the photosynthetic rate in grams C per gram C per day ($P_{I,C}$):

$$P_{I,C} = P_{I.chl} \times \text{chl}-a_C \times \frac{12\ \text{h}}{\text{day}} \times \frac{1\ \text{g}}{1000\ \text{mg}} \tag{2}$$

We used attack rate as a proxy for the mixotroph's investment in phagotrophy. As with photosynthetic investment, we scaled attack rate to *Ochromonas* cellular carbon:

$$\text{attack}_C(\text{mL per pg C per hr}) = \frac{\text{attack}_{\text{cell}}(\text{mL per Ochromonas cell per hr})}{C_{\text{cell}}(\text{pg C per Ochromonas cell})}. \tag{3}$$

Finally, we converted grazing rates into units of grams C per grams C per day, using an estimate of 113.6 fg C per bacterial cell obtained previously from our *Ochromonas* cultures (Lepori-Bui et al., 2022):

$$g_C = \frac{g_{\text{cell}}\ (\text{bacteria per Ochromonas cell per day})}{C_{\text{cell}}\ (\text{pg C per Ochromonas cell})} \times \frac{113.6\ \text{fg C}}{\text{bacterium}} \times \frac{1\ \text{pg}}{1000\ \text{fg}} \tag{4}$$

Using these carbon-scaled measurements, we then approximated carbon use efficiency as:

$$\text{CUE} = \frac{\text{growth rate}}{\text{total C obtained}} = \frac{\text{growth rate}}{\text{phototrophy} + \text{phagotrophy}} \tag{5}$$

where all rates are measured in units of grams C per grams C per day.

Phylogeny construction

To build a phylogeny, we amplified the partial 18S rRNA gene of all eight *Ochromonas* strains used in our study. For each strain, cells growing at 50 μmol photons · m^{-2} · s^{-1} were harvested by centrifugation at 8000 *g* for 10 min. DNA was extracted using a 2× Lysis/CTAB extraction (Gast et al., 2004). We performed PCR (Taq 2× master mix, New England BioLabs, Ipswich, MA) to amplify the 18S rRNA gene using the primers SSU1065F, SSU1954R (annealing temperature 49°C) and SSU1, SSU1295 (annealing temperature 57°C; Yang et al., 2012). Polymerase chain reaction conditions were: (1) denaturation at 95°C for 1 min, (2) 35 rounds of amplification (95°C for 1 min, annealing at 49°C for primer pair one and 57°C for primer pair two for 1 min, and elongation at 68°C for 1 min), and (3) a final step of 95°C for 2 min. Amplified PCR product was purified with a 1% Ampure bead solution (Beckman Coulter, Indianapolis, IN). Sanger sequencing was performed at MCLAB (South San Francisco, CA, USA). Sequences were trimmed and error corrected with Geneious Prime 2022.2.1 (https://www.geneious.com). A broad array of 18S rRNA gene sequences were downloaded from BLAST searches of our culture sequences on NCBI and aligned using the pairwise aligner tool in Mesquite (v. 3.61; Maddison & Maddison, 2023), followed by manual editing. A consensus phylogenetic tree was constructed using PhyML 3.0 (Guindon et al., 2010), using smart model selection (Lefort et al., 2017) for both Akaike and Bayesian information criteria, with 1000 bootstrap replications for each.

Statistical analyses and comparative phylogenetic methods

We conducted all statistical analyses using the programming language R (R Core Team, 2023). For

physiological comparisons, as appropriate to the statistical hypotheses being tested, we used *t*-tests and analysis of variance (ANOVA) tests to distinguish between means that differed from zero and means that differed across strains and/or treatments, respectively. When multiple hypotheses were tested using *t*-tests, we performed a Bonferroni correction for multiple hypothesis testing. When ANOVA tests were performed, we used Tukey's honestly significant difference post hoc tests to identify significant differences between groups while correcting for multiple hypothesis testing. We looked for tradeoffs in metabolic investments by comparing chlorophyll (a proxy for photosynthetic investment) and attack rates (a proxy for phagotrophic investment), and rates of photosynthetic and phagotrophic C acquisition, to test for negative relationships between investments and acquisition rates (Figure 1h).

We also tested, in two ways, the hypothesis that strains that were closely related phylogenetically had similar physiologies. First, we used comparative phylogenetic methods to ask whether more closely related species were more physiologically similar to one another by computing Blomberg's *K* (Münkemüller et al., 2012) using the function phylosig in the R package phytools (Revell, 2023). Second, we tested for correlations between genetic distance (i.e., number of different base pairs) and physiological distance (i.e., dissimilarity in physiological response to resource availability, measured as euclidean distance) using a Mantel test (Diniz-Filho et al., 2013) using the function mantel test in the R package ape (Paradis et al., 2023). However, because our strains were selected based on availability rather than selected to create a balanced phylogenetic design, we note that these results should be interpreted cautiously.

RESULTS

Growth rates increased with light and prey availability

All assayed strains of *Ochromonas* were mixotrophic with growth rates that increased with increases in light and prey availability (Figure 2). Generally, growth rates plateaued at high irradiance, but the growth-saturating irradiances varied by strain and food availability. For example, while most strains showed no increase (or even a decrease) in growth rates at irradiances above 75 μmol photons · m^{-2} · s^{-1}, some strains such as CCMP 584 and CCMP 1150 continued to increase their growth rates with light in low prey conditions. Strains also varied in their sensitivities to prey abundance (ordered in Figure 2 from largest increase in growth with prey to least). For example, the growth rate of CCMP 584 doubled in the high-prey treatment, while the growth rate of CCMP 1391 was relatively insensitive to prey abundance (growth rates at each light level were not significantly different from one another at the $p < 0.05$ level; two-sided *t*-test with Bonferroni correction for seven light levels = seven hypothesis tests). Five strains were able to grow in the absence of light when there was a surplus of prey available. However, strains in low prey conditions could not grow in darkness (0 μmol phoons · m^{-2} · s^{-1}), with the exception of CCMP 1393, which was able to maintain a significantly positive growth rate (Figure 2). Strains CCMP 1392, 1150, and 1391 appeared to be obligate phototrophs, as they could not achieve growth rates without light, even in the presence of ample prey (Figure 2).

Mixotroph growth rates increased with photosynthetic rates (Figure 3; See Appendix S1: Figure S3

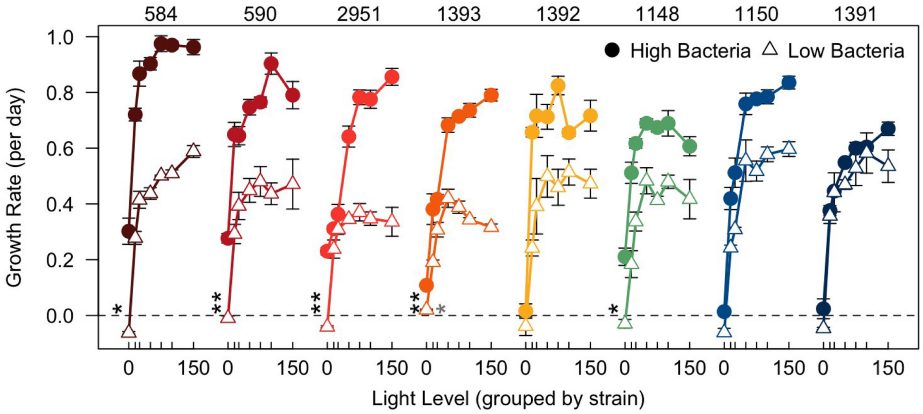

FIGURE 2 Effect of changing light levels on growth of eight *Ochromonas* strains under either high prey (closed circle) or low prey (open triangle) conditions acclimated to 0, 15, 25, 50, 75, 100, and 150 μmol photons · m^{-2} · s^{-1}. Strains are ordered from largest increase in growth with high bacterial availability to least. Error bars represent ±1 standard deviation among biological triplicates. Asterisks indicate Bonferroni-corrected *t*-tests of the hypothesis that growth rate in darkness exceeded zero. Black asterisks indicate statistical significance for high-prey treatments, and gray asterisks indicate statistical significance for low-prey treatments (*$p < 0.05$, **$p < 0.01$). [Color figure can be viewed at wileyonlinelibrary.com]

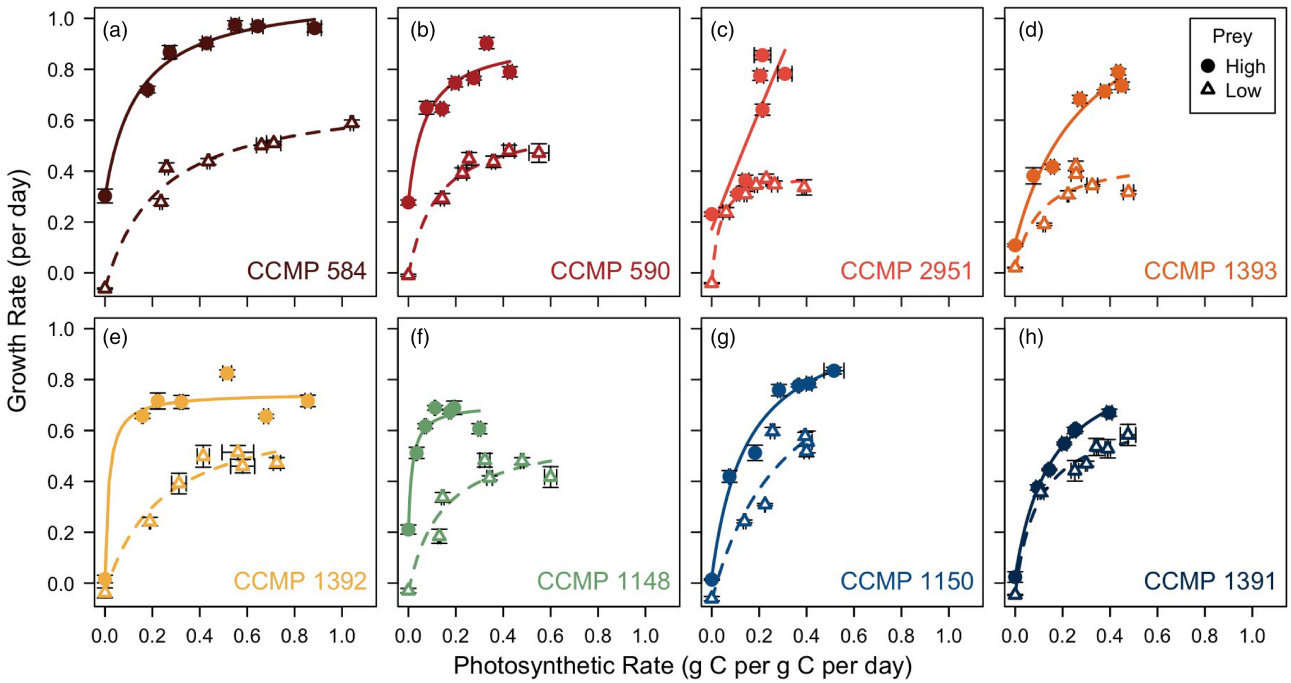

FIGURE 3 The relationship between growth rate (per day) and photosynthetic rate (g C per g C per day) of eight *Ochromonas* isolates under high prey (filled circles) and low prey (hollow triangles) conditions. Error bars represent ±1 standard deviation around the mean (points). Solid lines represent saturating functional response curve fits for high-prey isolates, while dashed lines represent the relationship for low-prey isolates. *Ochromonas* growth rates have a positive correlation with photosynthetic rates. [Color figure can be viewed at wileyonlinelibrary.com]

for growth as a function of grazing). However, growth rates were a saturating function of photosynthesis, suggesting that even when carbon supply from photosynthesis was abundant, another factor was likely limiting growth (Figure 3). Although all strains except CCMP 1391 achieved higher growth rates in high prey conditions (Figure 2), the estimated maximum growth rates achievable (asymptote of the saturating curve fits; Appendix S1: Figure S4) were only higher in high prey conditions for strains CCMP 584, 590, 1393, and 1391. These results suggest that if strains CCMP 1392, 1148, and 1150 could achieve higher photosynthetic rates in low-bacteria conditions, then they could increase their growth rates further. However, plateauing of growth rates with increasing light for these treatments suggests that light was not the growth-limiting factor (Figure 2; results were uncertain for CCMP 2951, due to a large error margin in the estimated maximum growth rate in the high prey treatment).

We also observed differences in carbon use efficiency depending on prey availability. Except for strain CCMP 1148, when mixotrophs had a surplus of prey, their carbon use efficiency decreased by up to a factor of 3 (Figure 4). *Ochromonas* cells were also physically larger (i.e., had higher cellular C and N content; Appendix S1: Figure S5) and tended to be more nutrient-dense (lower C:N ratios; Figure S5) in high-prey treatments. While these trends were present in all strains, they were only statistically significant in about half of the strains (Figure S5).

Metabolic investments vary with resource availability

All *Ochromonas* strains included in this study exhibited phenotypic plasticity in their metabolic investments in photosynthesis (chlorophyll content) and phagotrophy (attack rate). In both high prey and low prey conditions, all eight strains showed evidence of photoacclimation by decreasing their chlorophyll (pg per carbon) as light intensity increased (Figure 5a). However, all strains, regardless of prey condition, had their lowest amounts of chlorophyll (pg per carbon) in complete darkness.

All eight *Ochromonas* strains showed evidence that investments in both photosynthesis and phagotrophy declined with additional prey. In general, high-prey *Ochromonas* cultures invested less in chlorophyll content than their low-prey counterparts, excluding CCMP 2951, which had similar chlorophyll content for both high prey and low prey conditions (Figure 5a). In addition, the attack rates of strains in high prey treatments were lower than low prey treatments (Figure 5b). Despite these low attack rates, bacterial grazing rates were still highest in high prey treatments because of the relatively greater density of prey (Appendix S1: Figure S6).

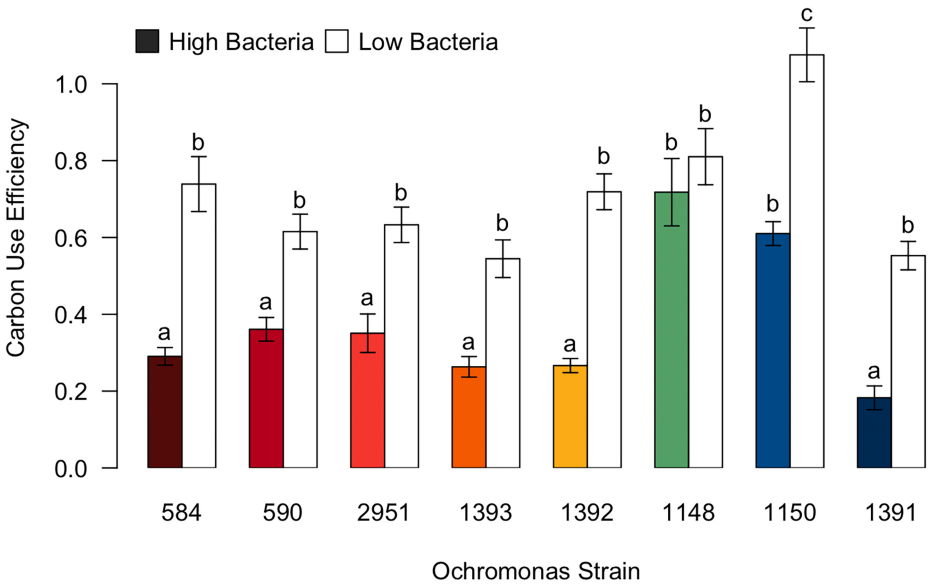

FIGURE 4 Carbon use efficiency for eight strains of *Ochromonas*. Strains in low prey conditions are represented without shading, while strains in high prey conditions are represented with darker color shading. All strains of *Ochromonas* in a low prey environment had a higher carbon use efficiency than those in a high-prey environment. Letters indicate statistically significant differences (Tukey's honestly significant difference test, $p < 0.05$). Bar heights are means, and error bars represent ±1 standard deviation. [Color figure can be viewed at wileyonlinelibrary.com]

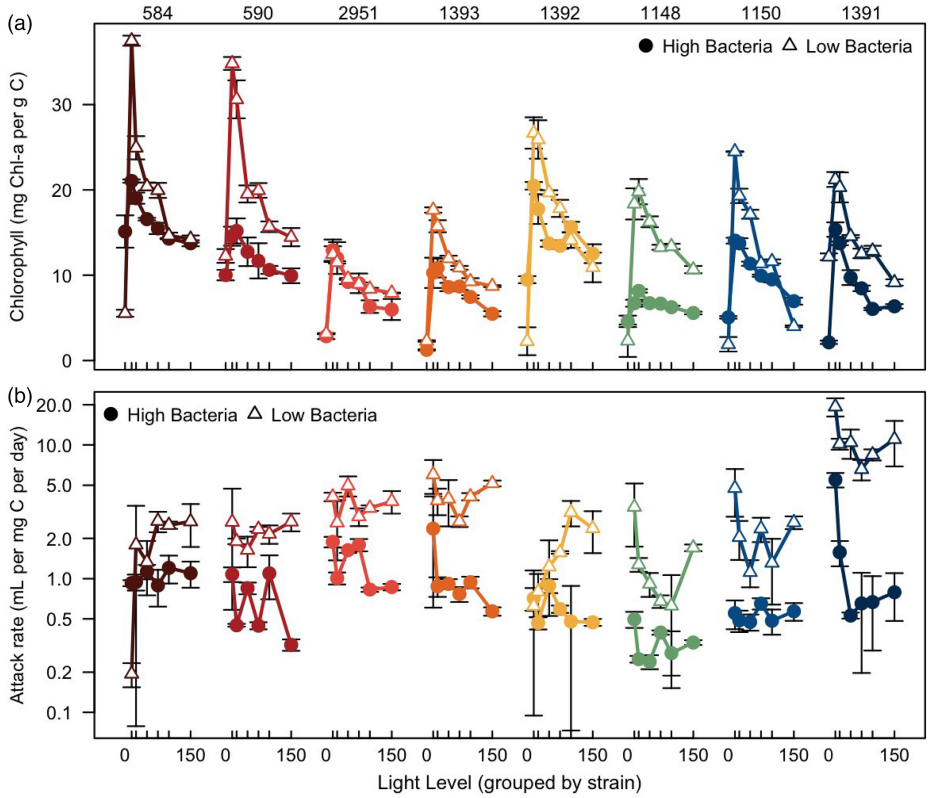

FIGURE 5 Metabolic investments in the eight *Ochromonas* isolates under high prey (closed circle) and low prey (open triangle) conditions are compared over a light gradient of 0–150 μmol photons · m^{-2} · s^{-1} (a) The effect of light level on chlorophyll content per carbon. Chlorophyll content per carbon is higher for low-prey *Ochromonas* isolates. All isolates exhibit a general decrease in chlorophyll content per carbon as light level increases. (b) The effect of light level on attack rate per carbon of *Ochromonas* isolates. Attack rate per carbon of *Ochronomas* isolates decreased with an increase in prey availability, but changes with light level were more variable. Note log scale of *y*-axis. Error bars represent ±1 standard deviation. [Color figure can be viewed at wileyonlinelibrary.com]

Relationships between growth, phototrophy, and phagotrophy

For most strains, as growth rate increased, investments in *both* photosynthesis and phagotrophy decreased simultaneously. For instance, strains CCMP 590, 1148, 1150, and 1391 had the highest growth rates when they invested the least in both photosynthesis and phagotrophy (Figure 6b,f,g,h). Two mixotrophs, strains CCMP 584 and 1392, exhibited evidence for tradeoffs between photosynthetic and phagotrophic investments, in which mixotrophs dedicate less energy to a less energetically favorable process (Figure 6a,e). For these strains, when growth rates were low, increased photosynthetic investments were coupled with decreased attack rates. These tradeoffs (i.e., decreases in chlorophyll content with increasing attack rates; Figure 1h) emerged only when cells were prey-limited. In addition, when prey was available for strain CCMP 1148, this strain showed a significant decrease in photosynthetic rate (g C per g C per d), implying there may be a tradeoff between photosynthesis and phagotrophy (Appendix S1: Figure S7f).

Most *Ochromonas* strains showed limited evidence for a correlation between carbon acquisition rates from phagotrophy and photosynthesis, whether positive or negative (Figure S7). The CCMP 584 and CCMP 1150 strains are exceptions, which showed slight positive correlations between carbon acquisition rates from phagotrophy and photosynthesis; CCMP 584 showed this correlation for both high and low-prey treatments, while CCMP 1150 showed this correlation for only high-prey treatments (Figure S7a,g). CCMP 1391 was the only strain to show similar carbon acquisition rates for both high and low prey treatments (Figure S7h).

We found limited evidence for synergies between photosynthesis and phagotrophy. Here, we define a synergistic effect as one that occurs when one mode of metabolism directly enhances the other (a stricter definition than the observance of an additive effect on growth of two forms of metabolism). For example, the photosynthetic efficiency and photosynthetic rate of strain CCMP 2951 increased with high-prey availability and higher grazing rates (Appendix S1: Figure S8). However, the photosynthetic efficiency and photosynthetic rate for all other strains were unchanged by a surplus of prey.

Ochromonas phylogenetic relatedness did not predict physiological similarity

The eight *Ochromonas* strains used in this study were distributed across the tree of existing *Ochromonas* sequences, and sequences from CCMP 584, 1393, and 2951 matched existing published sequences. Six of the eight strains were indistinguishable within the ca. 800 bp 18S rRNA region amplified (Figure 7), leaving us with limited statistical power to detect phylogenetic signal. Unsurprisingly given these constraints, we

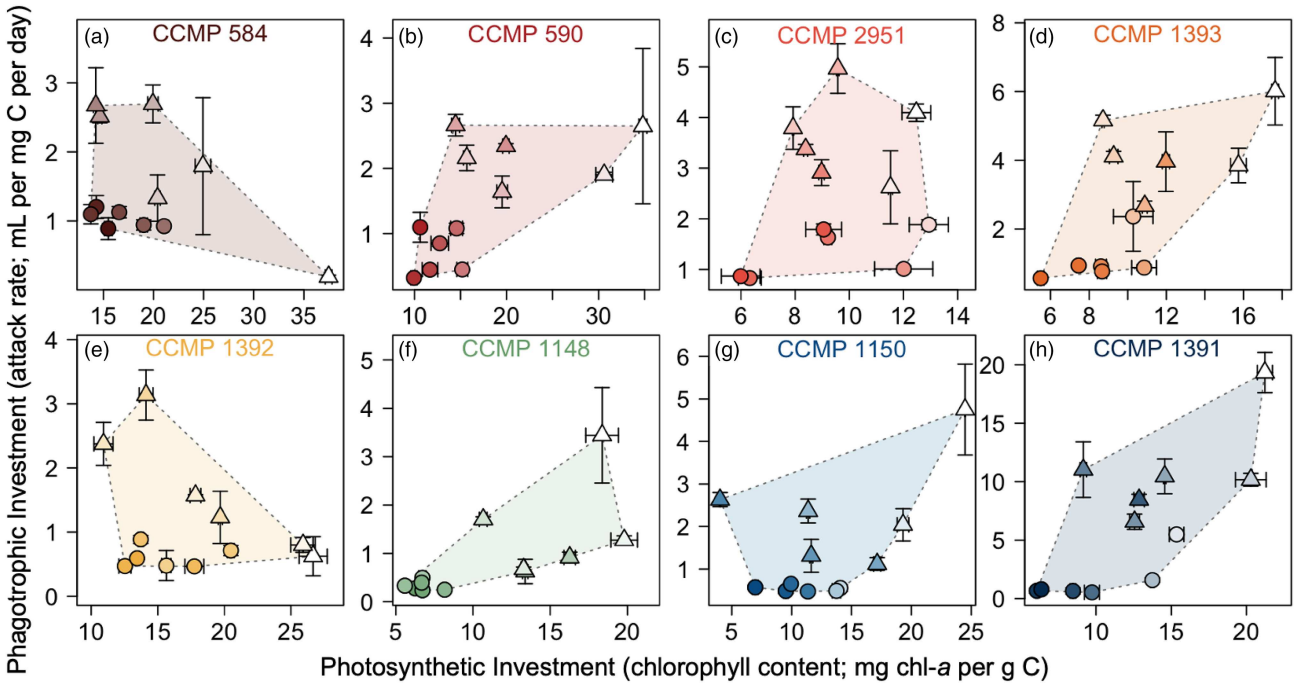

FIGURE 6 Photosynthetic investments (*x*-axis) compared to heterotrophic investments (*y*-axis) of *Ochromonas* under high-prey (circle) and low-prey (triangle) conditions. Color saturation is proportional to growth rate: More saturated (intensely colored) points indicate higher growth rates. Error bars represent ±1 standard deviation. Background shading represents the trait space occupied by each strain.

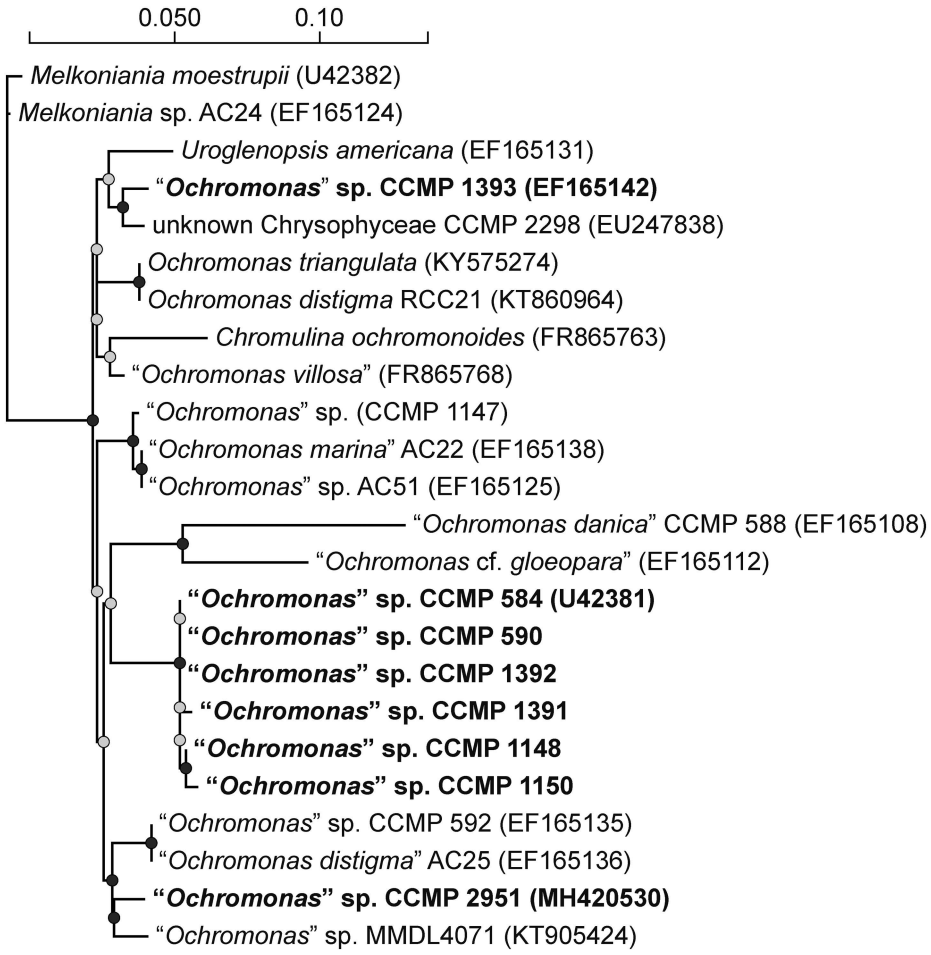

FIGURE 7 Phylogenetic tree of *Ochromonas* and closely related chrysophytes based on a partial 18S rRNA gene sequence. Taxon names are given in double quotation marks when identity as *Ochromonas* is uncertain, and GenBank sequence accession numbers are provided in parentheses for previously published sequences (including for strains CCMP 584, 1393, and 2951, used in this study). Strains typeset in bold font are those used in this experiment. Nodes indicate bootstrap support (black nodes show support in 500 or more out of 1000 bootstrap replicates).

found no relationship between phylogenetic distance or sequence dissimilarity and physiological performance. Specifically, all phylogenetic signal tests and Mantel tests yielded nonsignificant results (Appendix S1: Tables S2 and S3), suggesting that phylogeny and physiology were not clearly linked in the eight *Ochromonas* strains studied. This is consistent with observations of the data that showed relatively similar physiology in the more distantly related strains CCMP 2951 and 1393, in contrast to more variable physiology in the phylogenetically indistinguishable clade of the other six strains.

DISCUSSSION

In order to understand the role of mixotrophs in complex food webs and biogeochemical cycles, we analyzed the contributions of photosynthesis and phagotrophy to the metabolism of the constitutive mixotroph *Ochromonas* under various environmental conditions. We studied how light and prey-resource availability impacted the growth rates, energy acquisition rates, and investment strategies of eight strains from the genus *Ochromonas*. Our results showed that these mixotrophs vary in their metabolic strategies: Although all strains showed increased growth rates with increasing resource availability, some were obligate phototrophs that required light for growth (CCMP 1392, 1150, 1391), whereas some showed stronger metabolic responses to prey availability (CCMP 584, 590, 2951, 1393, 1148; Figure 2). All our *Ochromonas* strains varied their metabolic investments as a function of environmental conditions, tending to upregulate photosynthetic machinery when light was limiting and increase attack rates when bacterial abundances were low (Figure 5). Other studies have shown that mixotrophic species vary their metabolic investment depending on available resources. For instance, photoacclimation, via reduction in chlorophyll-*a* content and photosynthetic efficiency with light, has been observed in mixotrophic dinoflagellates (Coats & Harding Jr., 1988; Harding Jr., 1988). There is also evidence that mixotrophic species vary their investment

in photosynthesis as heterotrophic resources increase. Lewitus et al. (1991) observed that in sufficient light, the mixotrophic chrysophyte *Pyrenomonas salina* decreased chloroplast thylakoids as glycerol was added to cultures. In addition, Wilken et al. (2020) observed that *Ochromonas* strains decreased ingestion rates under limiting light levels. Collectively, our data are consistent with others' findings that mixotrophs adjust their metabolic investments in response to the resource landscape.

Our results show that mixotrophs photoacclimated to higher light levels by decreasing chlorophyll content. This photoacclimation strategy is consistent with "true phytoplankton," for which metabolism is dependent solely on photosynthesis (Dubinsky & Stambler, 2009). This strategy remained true for all our mixotrophic strains regardless of bacterial concentration. At the highest light levels used in our study, however, mixotrophs exhibited plateaus in photosynthetic carbon acquisition (Figure 3), especially in low-bacteria treatments, and (in some cases) declining growth rates (Figure 2). In part, this may be because of nutrient limitation due to low-prey availability. Although some *Ochromonas* strains appear to be able to assimilate inorganic nitrogen (Lie et al., 2018) and the K media used in this study has relatively high concentrations of nitrate and ammonium (Table S1), we also observed higher C:N ratios in low-prey treatments (Figure S5) consistent with the hypothesis of nutrient limitation in low-prey treatments. Under long-term exposure to very high light levels, mixotroph growth rates tend to decline (Wilken et al., 2020); our declines in growth rate at more modest light levels may be early indications of this trend.

In total darkness, all our *Ochromonas* strains and bacterial treatments exhibited reduced chlorophyll content. There are at least two explanations for this. First, the *Ochromonas* cells may have been reducing investment in a less profitable form of metabolism and prioritizing investment in heterotrophy. We saw evidence that investment in heterotrophy did increase in complete darkness for strains CCMP 1393, 1148, 1150, and 1391 in high-prey and low-prey conditions (Figure 5b). Therefore, when light levels increased, these strains acclimated by decreasing their attack rate per carbon investment and simultaneously increasing their investment in chlorophyll per carbon (Figure 5). Second, the *Ochromonas* cells may have been unable to produce chlorophyll in darkness either because of light-requiring steps in pigment biosynthesis (Castelfranco & Beale, 1981) or because the cells were experiencing negative growth rates and were generally in decline. In all cases, our bacteria-limited *Ochromonas* had negative or near-zero growth rates in darkness; chlorophyll content data from these strains are therefore not a very reliable indicator of steady state physiological performance.

Metabolic investment strategies were dependent on resource availability. When growth rates were high, all *Ochromonas* strains tended to reduce their per carbon investments in both forms of metabolism. However, it is interesting to note that when growth rates were low and chlorophyll content was high, strains CCMP 584 and CCMP 1392 showed reduced investment in phagotrophy (Figure 6a,e). We hypothesize that *Ochromonas* strains may be optimizing a more complex set of investments than simply photosynthesis and phagotrophy. For example, if *Ochromonas* growth rates are proportional to investment in some other cellular structure, such as growth (reproduction) machinery (Clark et al., 2013), then when supplies of carbon and nutrients from photosynthesis and phagotrophy are high, *Ochromonas* cells should reduce investment in photosynthesis and phagotrophy in favor of greater investment in reproduction. The existence of other growth-limiting factors is supported by our observation that *Ochromonas* growth rates saturated at high resource availability, even though rates of carbon acquisition (through photosynthesis and grazing) continued to increase (Figure 4, Figure S7). This resulted in the emergence of a "Pareto frontier" for strains CCMP 584 and CCMP 1392 (Figure 6). Pareto frontiers are boundaries (here, tradeoffs) between constraints (here, investments in phototrophy and phagotrophy) that only emerge when other constraints (here, investments in growth machinery) are relaxed (Mattson & Messac, 2005). For strains CCMP 584 and CCMP 1392, the tradeoff between photosynthesis and phagotrophy is only apparent when resource acquisition is the limiting factor or, in other words, when growth rates are low (Figure 6). However, frontiers did not appear for all strains. This may be because evolutionary constraints, or other cellular investments not measured in this study, limited the extent to which *Ochromonas* cells could decouple photosynthesis and phagotrophy.

Findings from other studies are consistent with our evidence that mixotrophic strains vary in the extent of their metabolic tradeoffs. For instance, Lie et al. (2018) showed that the *Ochromonas* strain CCMP 1393 did not experience metabolic tradeoffs. Instead, CCMP 1393 increased expression of over half of the genes for photosystem proteins when prey was available (Lie et al., 2018); however, *Ochromonas* strain BG-1 did downregulate light harvesting and carbon fixation when prey was available, suggesting a tradeoff. Wilken et al. (2020) confirmed the interdependency of photosynthesis and phagotrophy in strain CCMP 1393 and partially substitutable routes for metabolism in strain CCMP 2951. Additionally, some *Ochromonas* strains have been shown to produce accessory photo-protective pigments including fucoxanthin, carotene, and diadinoxanthin (Wilken et al., 2020), which we did not measure in this study.

Therefore, the decrease in chlorophyll content does not necessarily mean there was energy available to invest in phagotrophy, potentially obscuring tradeoffs. We also did not identify the exact phagotrophic modes of the *Ochromonas* strains in our study. Some *Ochromonas* species, such as *O. danica*, create a flagella-induced current to pull prey towards the cell (Aaronson & Behrens, 1973). This phagotrophic strategy is more energetically costly than the more passive phagotrophic strategy, so variation in strategies across strains could explain differences in observed tradeoffs. Overall, better measurements of additional cellular investments are needed to further understand how mixotrophic physiology changes with resource availability.

In our study, photosynthesis and phagotrophy generally produced additive benefits. In the presence of additional bacterial prey, *Ochromonas* growth rates were elevated above the maximum, light-saturated rates of growth at lower bacterial abundances (Figure 2). This suggests that there is some difference in nutritional yield from phagotrophy that can support more rapid growth. This could be due to acquisition of noncarbon nutrients, metabolically expensive metabolites, or other growth factors. For example, in the presence of prey, *Ochromonas* strain CCMP 1393 is known to upregulate genes associated with ammonium assimilation and the urea cycle by 50% (Lie et al., 2018). There is also evidence that the primary phagotrophic function for other mixotrophic chrysophytes is to provide nutrients such as nitrogen and phospholipid requirements (Caron et al., 1993; Kimura & Ishida, 1989). Nonsubstitutability of metabolism may also arise from different efficiencies of assimilating resources from ingested prey compared to photosynthetically derived carbohydrates. For instance, some *Ochromonas* species have been shown to be unable to efficiently use dissolved organic carbon for growth, as they have negative growth rates in low light conditions despite ample phagotrophic resources (Fischer et al., 2022). Thus, photosynthesis and phagotrophy may, to some extent, provide "non-substitutable" forms of resources for the mixotroph (Tilman, 1980).

We found limited evidence for synergies between the two forms of metabolism. Well-fed mixotrophs tended to reduce their investments in photosynthetic machinery. Therefore, even though photosynthetic efficiencies and per-chlorophyll rates were sometimes higher in high-bacteria cultures, overall photosynthetic rates tended to be similar to or lower than those in low-bacteria cultures. In addition, there was limited evidence for a correlation between carbon acquisition rates from photosynthesis or phagotrophy. However, we did not measure flows of nutrients within the mixotroph cells, so it is still possible that nutrients such as N and P or other micronutrients obtained from phagotrophy supported the production of photosynthetic machinery (Flynn & Mitra, 2009). Studies have shown that *Ochromonas* strains can obtain 88%–95% of nitrogen from phagotrophy (Terrado et al., 2017), and phagotrophic ingestion of bacteria can allow *Ochromonas* to acquire iron for the use in photosynthetic metabolic reactions (Maranger et al., 1998). We also did not measure nutrient cycling in the community, which means that another potential synergy—in which C exuded by *Ochromonas* fuels bacterial growth and, in turn, additional phagotrophy—may also have gone unnoticed in our experiments. Our inference is also limited by how we measured investment in phagotrophy. We used attack rate as a proxy for investment in digestive vacuoles; future studies could use vacuole counts or phagotrophic gene upregulation as alternate measurements for heterotrophic investment.

We also found limited evidence that phylogenetic relatedness is correlated with similarity of physiological responses to resource availability or metabolic strategy among our eight *Ochromonas* strains (Figure 7). Although such findings suggest that it may be difficult to predict mixotroph phenotype from, for example, barcoding, we emphasize that our phylogenetic analysis has a number of important limitations. First, our study was not designed to test for phylogenetic signal: Our strains were selected opportunistically based on availability in a culture collection, and did not represent a phylogenetically balanced design. Second, the *Ochromonas* genus is polyphyletic and, in general, the tree is poorly resolved (Andersen et al., 2017; Lie et al., 2018). Our own sequencing data was also limited, which meant that it was difficult to robustly position our strains on the phylogeny. Thus, it is difficult to draw meaningful conclusions about how metabolic strategies may have evolved within the genus based on our results.

In summation, our results highlight how environmental conditions affect the mixotrophic metabolic strategies of *Ochromonas*. There were a variety of metabolic responses to resource availability between each strain of *Ochromonas*. Recognizing the variation of metabolism between different mixotrophic strains will help us understand the many ways in which mixotrophs may affect ecological processes, community interactions, and carbon cycling.

AUTHOR CONTRIBUTIONS

Gina S. Barbaglia: Conceptualization (supporting); data curation (equal); formal analysis (equal); funding acquisition (supporting); investigation (lead); methodology (supporting); visualization (supporting); writing – original draft (equal); writing – review and editing (equal). **Christopher Paight:** Formal analysis (supporting); investigation (supporting); methodology (supporting); supervision (supporting); writing – review and

editing (supporting). **Meredith Honig:** Investigation (supporting); writing – review and editing (supporting). **Matthew D. Johnson:** Formal analysis (supporting); writing – review and editing (supporting). **Ryan Marczak:** Investigation (supporting); writing – review and editing (supporting). **Michelle Lepori-Bui:** Methodology (supporting); writing – review and editing (supporting). **Holly V. Moeller:** Conceptualization (lead); data curation (equal); formal analysis (equal); funding acquisition (lead); investigation (supporting); methodology (lead); project administration (lead); resources (lead); supervision (lead); validation (lead); visualization (lead); writing – original draft (equal); writing – review and editing (equal).

ACKNOWLEDGMENTS

The authors would like to thank the members of the Moeller Laboratory group at UC Santa Barbara, Todd Oakley, Adrian Stier, Kathryn Cottingham, and four anonymous reviewers for their comments and feedback. This research was supported by a UC Santa Barbara Undergraduate Research & Creative Activities grant to Gina S. Barbaglia, by the US National Science Foundation (OCE-1851194 and OCE-2237017 to HVM), and by the Simons Foundation (Award 689265 to HVM).

CONFLICT OF INTEREST STATEMENT

None declared.

DATA AVAILABILITY STATEMENT

Data files and analysis code are available on GitHub at doi: 10.5281/zenodo.10247147.

ORCID

Gina S. Barbaglia https://orcid.org/0000-0002-7092-2620
Holly V. Moeller https://orcid.org/0000-0002-9335-0039

REFERENCES

Aaronson, S., & Behrens, U. (1973). A note on the fine structure of the Ochromonas danica "tail." *Archiv für Mikrobiologie*, *93*(4), 359–362. https://doi.org/10.1007/BF00427931

Andersen, R. A., Graf, L., Malakhov, Y., & Yoon, H. S. (2017). Rediscovery of the *Ochromonas* type species *Ochromonas triangulata* (Chrysophyceae) from its type locality (Lake Veysove, Donetsk region, Ukraine). *Phycologia*, *56*(6), 591–604. https://doi.org/10.2216/17-15.1

Andersson, A., Falk, S., Samuelsson, G., & Hagström, Å. (1989). Nutritional characteristics of a mixotrophic nanoflagellate, *Ochromonas* sp. *Microbial Ecology*, *17*(3), 251–262. https://doi.org/10.1007/BF02012838

Berge, T., Chakraborty, S., Hansen, P. J., & Andersen, K. H. (2017). Modeling succession of key resource-harvesting traits of mixotrophic plankton. *The ISME Journal*, *11*(1), 212–223. https://doi.org/10.1038/ismej.2016.92

Caron, D. A. (2016). Mixotrophy stirs up our understanding of marine food webs. *Proceedings of the National Academy of Sciences of the United States of America*, *113*(11), 2806–2808. https://doi.org/10.1073/pnas.1600718113

Caron, D. A., Sanders, R. W., Lim, E. L., Marrasé, C., Amaral, L. A., Whitney, S., Aoki, R. B., & Porters, K. G. (1993). Light-dependent phagotrophy in the freshwater mixotrophic chrysophyte *Dinobryon cylindricum*. *Microbial Ecology*, *25*(1), 93–111. https://doi.org/10.1007/BF00182132

Castelfranco, P. A., & Beale, S. I. (1981). 9—Chlorophyll biosynthesis. In M. D. Hatch & N. K. Boardman (Eds.), *Photosynthesis* (pp. 375–421). Academic Press. https://doi.org/10.1016/B978-0-12-675408-7.50015-X

Clark, J. R., Lenton, T. M., Williams, H. T. P., & Daines, S. J. (2013). Environmental selection and resource allocation determine spatial patterns in picophytoplankton cell size. *Limnology and Oceanography*, *58*(3), 1008–1022. https://doi.org/10.4319/lo.2013.58.3.1008

Coats, D. W., & Harding, L. W., Jr. (1988). Effect of light history on the ultrastructure and physiology of *Prorocentrum mariae-lebouriae* (Dinophyceae). *Journal of Phycology*, *24*(1), 67–77. https://doi.org/10.1111/j.1529-8817.1988.tb04457.x

Diniz-Filho, J. A. F., Soares, T. N., Lima, J. S., Dobrovolski, R., Landeiro, V. L., Telles, M. P. d. C., Rangel, T. F., & Bini, L. M. (2013). Mantel test in population genetics. *Genetics and Molecular Biology*, *36*, 475–485. https://doi.org/10.1590/S1415-47572013000400002

Dubinsky, Z., & Stambler, N. (2009). Photoacclimation processes in phytoplankton: Mechanisms, consequences, and applications. *Aquatic Microbial Ecology*, *56*(2–3), 163–176. https://doi.org/10.3354/ame01345

Escoubas, J. M., Lomas, M., LaRoche, J., & Falkowski, P. G. (1995). Light intensity regulation of cab gene transcription is signaled by the redox state of the plastoquinone pool. *Proceedings of the National Academy of Sciences of the United States of America*, *92*(22), 10237–10241.

Estep, K. W., Davis, P. G., Keller, M. D., & Sieburth, J. M. N. (1986). How important are oceanic algal nanoflagellates in bacterivory? *Limnology and Oceanography*, *31*(3), 646–650. https://doi.org/10.4319/lo.1986.31.3.0646

Falkowski, P. G. (1980). Light-shade adaptation in marine phytoplankton. In P. G. Falkowski (Ed.), *Primary productivity in the sea* (pp. 99–119). Springer. https://doi.org/10.1007/978-1-4684-3890-1_6

Falkowski, P. G., Owens, T. G., Ley, A. C., & Mauzerall, D. C. (1981). Effects of growth irradiance levels on the ratio of reaction centers in two species of marine phytoplankton. *Plant Physiology*, *68*(4), 969–973. https://doi.org/10.1104/pp.68.4.969

Fischer, R., Kitzwögerer, J., & Ptacnik, R. (2022). Light-dependent niche differentiation in two mixotrophic bacterivores. *Environmental Microbiology Reports*, *14*(4), 530–537. https://doi.org/10.1111/1758-2229.13071

Flynn, K. J., & Mitra, A. (2009). Building the "perfect beast": Modelling mixotrophic plankton. *Journal of Plankton Research*, *31*(9), 965–992. https://doi.org/10.1093/plankt/fbp044

Foster, B. L. L., & Chrzanowski, T. H. (2012). The mixotrophic protist *Ochromonas danica* is an indiscriminant predator whose fitness is influenced by prey type. *Aquatic Microbial Ecology*, *68*(1), 1–11. https://doi.org/10.3354/ame01594

Gast, R. J., Dennett, M. R., & Caron, D. A. (2004). Characterization of protistan assemblages in the Ross Sea, Antarctica, by denaturing gradient gel electrophoresis. *Applied and Environmental Microbiology*, *70*(4), 2028–2037. https://doi.org/10.1128/AEM.70.4.2028-2037.2004

Gorbunov, M. Y., & Falkowski, P. G. (2005). Fluorescence induction and relaxation (FIRe) technique and instrumentation for monitoring photosynthetic processes and primary production

in aquatic ecosystems. In A. van der ESt, & B. Bruce (Eds.), *Photosynthesis: Fundamental aspects to global perspectives – Proceedings of the 13th International Congress of Photosynthesis* (Vol. *2*, pp. 1029–1031). Allen Press.

Guindon, S., Dufayard, J.-F., Lefort, V., Anisimova, M., Hordijk, W., & Gascuel, O. (2010). New algorithms and methods to estimate maximum-likelihood phylogenies: Assessing the performance of PhyML 3.0. *Systematic Biology*, *59*(3), 307–321. https://doi.org/10.1093/sysbio/syq010

Harding, L. W., Jr. (1988). The time-course of photoadaptation to low-light in *Prorocentrum mariae-lebouriae* (Dinophyceae). *Journal of Phycology*, *24*(2), 274–281. https://doi.org/10.1111/j.1529-8817.1988.tb04243.x

Hartmann, M., Grob, C., Tarran, G. A., Martin, A. P., Burkill, P. H., Scanlan, D. J., & Zubkov, M. V. (2012). Mixotrophic basis of Atlantic oligotrophic ecosystems. *Proceedings of the National Academy of Sciences of the United States of America*, *109*(15), 5756–5760. https://doi.org/10.1073/pnas.1118179109

Holen, D. (2010). Mixotrophy in two species of *Ochromonas*. *Nova Hedwigia, Beiheft*, *136*, 153–165.

Jansson, M., Blomqvist, P., Jonsson, A., & Bergström, A.-K. (1996). Nutrient limitation of bacterioplankton, autotrophic and mixotrophic phytoplankton, and heterotrophic nanoflagellates in Lake Örträsket. *Limnology and Oceanography*, *41*(7), 1552–1559. https://doi.org/10.4319/lo.1996.41.7.1552

Jassby, A. D. & Platt, T. (1976). Mathematical formulation of the relationship between photosynthesis and light for phytoplankton. *Limnology and Oceanography*, *21*(4), 540–547. https://doi.org/10.4319/lo.1976.21.4.0540

Jassey, V. E. J., Signarbieux, C., Hättenschwiler, S., Bragazza, L., Buttler, A., Delarue, F., Fournier, B., Gilbert, D., Laggoun-Défarge, F., Lara, E., Mills, R. T. E., Mitchell, E. A. D., Payne, R. J., & Robroek, B. J. M. (2015). An unexpected role for mixotrophs in the response of peatland carbon cycling to climate warming. *Scientific Reports*, *5*, 16931. https://doi.org/10.1038/srep16931

Jeong, H. J., & Latz, M. I. (1994). Growth and grazing rates of the heterotrophic dinoflagellates *Protoperidinium* spp. on red tide dinoflagellates. *Marine Ecology Progress Series*, *106*(1/2), 173–185.

Keller, M. D., Selvin, R. C., Claus, W., & Guillard, R. R. L. (1987). Media for the culture of oceanic ultraphytoplankton. *Journal of Phycology*, *23*(4), 633–638. https://doi.org/10.1111/j.1529-8817.1987.tb04217.x

Kimura, B., & Ishida, Y. (1989). Phospholipid as a growth factor of *Uroglena americana*, a red tide Chrysophyceae in Lake Biwa. *Nippon Suisan Gakkaishi*, *55*(5), 799–804. https://doi.org/10.2331/suisan.55.799

Lawrenz, E., Silsbe, G., Capuzzo, E., Ylöstalo, P., Forster, R. M., Simis, S. G. H., Prášil, O., Kromkamp, J. C., Hickman, A. E., Moore, C. M., Forget, M.-H., Geider, R. J., & Suggett, D. J. (2013). Predicting the electron requirement for carbon fixation in seas and oceans. *PLoS ONE*, *8*(3), e58137. https://doi.org/10.1371/journal.pone.0058137

Laws, E. A. (1991). Photosynthetic quotients, new production and net community production in the open ocean. *Deep Sea Research Part A. Oceanographic Research Papers*, *38*(1), 143–167. https://doi.org/10.1016/0198-0149(91)90059-O

Lefort, V., Longueville, J.-E., & Gascuel, O. (2017). SMS: Smart model selection in PhyML. *Molecular Biology and Evolution*, *34*(9), 2422–2424. https://doi.org/10.1093/molbev/msx149

Lepori-Bui, M., Paight, C., Eberhard, E., Mertz, C. M., & Moeller, H. V. (2022). *Evidence for evolutionary adaptation of mixotrophic nanoflagellates to warmer temperatures*. *bioRxiv* https://doi.org/10.1101/2022.02.03.479051

Lewitus, A. J., Caron, D. A., & Miller, K. R. (1991). Effects of light and glycerol on the organization of the photosynthetic apparatus in the facultative heterotroph *Pyrenomonas salina* (Cryptophyceae). *Journal of Phycology*, *27*(5), 578–587. https://doi.org/10.1111/j.0022-3646.1991.00578.x

Li, Q., Edwards, K., Schvarcz, C., Selph, K., & Steward, G. (2021). Plasticity in the grazing ecophysiology of *Florenciella* (Dichtyochophyceae), a mixotrophic nanoflagellate that consumes *Prochlorococcus* and other bacteria. *Limnology and Oceanography*, *66*, 47–60. https://doi.org/10.1002/lno.11585

Lie, A. A. Y., Liu, Z., Terrado, R., Tatters, A. O., Heidelberg, K. B., & Caron, D. A. (2018). A tale of two mixotrophic chrysophytes: Insights into the metabolisms of two *Ochromonas* species (Chrysophyceae) through a comparison of gene expression. *PLoS ONE*, *13*(2), e0192439. https://doi.org/10.1371/journal.pone.0192439

MacIntyre, H. L., Kana, T. M., Anning, T., & Geider, R. J. (2002). Photoacclimation of photosynthesis irradiance response curves and photosynthetic pigments in microalgae and cyanobacteria. *Journal of Phycology*, *38*(1), 17–38. https://doi.org/10.1046/j.1529-8817.2002.00094.x

Maddison, W. P., & Maddison, D. R. (2023). *Mesquite: A modular system for evolutionary analysis* (3.81) [computer software]. http://www.mesquiteproject.org

Maranger, R., Bird, D. F., & Price, N. M. (1998). Iron acquisition by photosynthetic marine phytoplankton from ingested bacteria. *Nature*, *396*(6708), 248–251. https://doi.org/10.1038/24352

Mattson, C. A., & Messac, A. (2005). Pareto frontier based concept selection under uncertainty, with visualization. *Optimization and Engineering*, *6*(1), 85–115. https://doi.org/10.1023/B:OPTE.0000048538.35456.45

Mitra, A., Flynn, K. J., Tillmann, U., Raven, J. A., Caron, D., Stoecker, D. K., Not, F., Hansen, P. J., Hallegraeff, G., Sanders, R., Wilken, S., McManus, G., Johnson, M., Pitta, P., Våge, S., Berge, T., Calbet, A., Thingstad, F., Jeong, H. J., … Lundgren, V. (2016). Defining planktonic protist functional groups on mechanisms for energy and nutrient acquisition: Incorporation of diverse mixotrophic strategies. *Protist*, *167*(2), 106–120. https://doi.org/10.1016/j.protis.2016.01.003

Moeller, H. V., Neubert, M. G., & Johnson, M. D. (2019). Intraguild predation enables coexistence of competing phytoplankton in a well-mixed water column. *Ecology*, *100*(12), e02874. https://doi.org/10.1002/ecy.2874

Münkemüller, T., Lavergne, S., Bzeznik, B., Dray, S., Jombart, T., Schiffers, K., & Thuiller, W. (2012). How to measure and test phylogenetic signal. *Methods in Ecology and Evolution*, *3*(4), 743–756. https://doi.org/10.1111/j.2041-210X.2012.00196.x

Paradis, E., Blomberg, S., Bolker, B., Brown, J., Claramunt, S., Claude, J., Cuong, H. S., Desper, R., Didier, G., Durand, B., Dutheil, J., Ewing, R. J., Gascuel, O., Guillerme, T., Heibl, C., Ives, A., Jones, B., Krah, F., … de Vienne, D. (2023). *ape: Analyses of Phylogenetics and Evolution* (5.7–1) [Computer software]. https://cran.r-project.org/web/packages/ape/

R Core Team. (2023). *R: A language and environment for statistical computing* [computer software]. R Foundation for Statistical Computing https://www.R-project.org/

Raven, J. A. (1997). Phagotrophy in phototrophs. *Limnology and Oceanography*, *42*(1), 198–205. https://doi.org/10.4319/lo.1997.42.1.0198

Revell, L. J. (2023). *Phytools: Phylogenetic tools for comparative biology (and other things)* (1.9-16) [computer software]. https://cran.r-project.org/web/packages/phytools/index.html

Sanders, R. W., Caron, D. A., Davidson, J. M., Dennett, M. R., & Moran, D. M. (2001). Nutrient acquisition and population growth of a mixotrophic alga in axenic and bacterized cultures. *Microbial Ecology*, *42*(4), 513–523. https://doi.org/10.1007/s00248-001-1024-6

Sanders, R. W., Porter, K. G., Bennett, S. J., & DeBiase, A. E. (1989). Seasonal patterns of bacterivory by flagellates, ciliates,

rotifers, and cladocerans in a freshwater planktonic community. *Limnology and Oceanography*, *34*(4), 673–687. https://doi.org/10.4319/lo.1989.34.4.0673

Sanders, R. W., Porter, K. G., & Caron, D. A. (1990). Relationship between phototrophy and phagotrophy in the mixotrophic chrysophyte *Poterioochromonas malhamensis*. *Microbial Ecology*, *19*(1), 97–109. https://doi.org/10.1007/BF02015056

Schmidtke, A., Bell, E. M., & Weithoff, G. (2006). Potential grazing impact of the mixotrophic flagellate *Ochromonas* sp. (Chrysophyceae) on bacteria in an extremely acidic lake. *Journal of Plankton Research*, *28*(11), 991–1001. https://doi.org/10.1093/plankt/fbl034

Stoecker, D. K. (1998). Conceptual models of mixotrophy in planktonic protists and some ecological and evolutionary implications. *European Journal of Protistology*, *34*(3), 281–290. https://doi.org/10.1016/S0932-4739(98)80055-2

Sukenik, A., Bennett, J., & Falkowski, P. (1988). Changes in the abundance of individual apoproteins of light-harvesting chlorophyll ab-protein complexes of photosystem I and II with growth irradiance in the marine chlorophyte *Dunaliella tertiolecta*. *Biochimica et Biophysica Acta (BBA)—Bioenergetics*, *932*, 206–215. https://doi.org/10.1016/0005-2728(88)90157-0

Terrado, R., Pasulka, A. L., Lie, A. A.-Y., Orphan, V. J., Heidelberg, K. B., & Caron, D. A. (2017). Autotrophic and heterotrophic acquisition of carbon and nitrogen by a mixotrophic chrysophyte established through stable isotope analysis. *The ISME Journal*, *11*(9), Article 9–Article 2034. https://doi.org/10.1038/ismej.2017.68

Tilman, D. (1980). Resources: A graphical-mechanistic approach to competition and predation. *The American Naturalist*, *116*(3), 362–393.

Våge, S., Castellani, M., Giske, J., & Thingstad, T. F. (2013). Successful strategies in size structured mixotrophic food webs. *Aquatic Ecology*, *47*(3), 329–347. https://doi.org/10.1007/s10452-013-9447-y

Ward, B. A., Dutkiewicz, S., Barton, A. D., & Follows, M. J. (2011). Biophysical aspects of resource acquisition and competition in algal mixotrophs. *The American Naturalist*, *178*(1), 98–112. https://doi.org/10.1086/660284

Wilken, S., Choi, C. J., & Worden, A. Z. (2020). Contrasting mixotrophic lifestyles reveal different ecological niches in two closely related marine protists. *Journal of Phycology*, *56*(1), 52–67. https://doi.org/10.1111/jpy.12920

Wilken, S., Schuurmans, J. M., & Matthijs, H. C. P. (2014). Do mixotrophs grow as photoheterotrophs? Photophysiological acclimation of the chrysophyte *Ochromonas danica* after feeding. *New Phytologist*, *204*(4), 882–889. https://doi.org/10.1111/nph.12975

Wilken, S., Yung, C. C. M., Hamilton, M., Hoadley, K., Nzongo, J., Eckmann, C., Corrochano-Luque, M., Poirier, C., & Worden, A. Z. (2019). The need to account for cell biology in characterizing predatory mixotrophs in aquatic environments. *Philosophical Transactions of the Royal Society B: Biological Sciences*, *374*(1786), 20190090. https://doi.org/10.1098/rstb.2019.0090

Yang, E. C., Boo, G. H., Kim, H. J., Cho, S. M., Boo, S. M., Andersen, R. A., & Yoon, H. S. (2012). Supermatrix data highlight the phylogenetic relationships of photosynthetic stramenopiles. *Protist*, *163*(2), 217–231. https://doi.org/10.1016/j.protis.2011.08.001

Zubkov, M. V., & Tarran, G. A. (2008). High bacterivory by the smallest phytoplankton in the North Atlantic Ocean. *Nature*, *455*(7210), 224–226. https://doi.org/10.1038/nature07236

SUPPORTING INFORMATION

Additional supporting information can be found online in the Supporting Information section at the end of this article.

Appendix S1: File containing Tables S1–S3 and Figures S1–S8.

How to cite this article: Barbaglia, G. S., Paight, C., Honig, M., Johnson, M. D., Marczak, R., Lepori-Bui, M., & Moeller, H. V. (2024). Environment-dependent metabolic investments in the mixotrophic chrysophyte *Ochromonas*. *Journal of Phycology*, *60*, 170–184. https://doi.org/10.1111/jpy.13418